Journal of Applied Polymer Science

REVIEW

Recent Advances on Polymer-Stabilized Blue Phase Liquid Crystal Materials and Devices

Yuan Chen, Shin-Tson Wu
CREOL, The College of Optics and Photonics, University of Central Florida, Orlando, Florida 32816
Correspondence to: S.-T. Wu (E-mail: swu@ucf.edu).

ABSTRACT: Polymer-stabilized blue phase liquid crystals (PS-BPLC) have become an increasingly important technology trend for information display and photonics applications. BPLCs exhibit several attractive features, such as reasonably wide temperature range, submillisecond gray-to-gray response time, no need for alignment layer, optically isotropic voltage-off state, and large cell gap tolerance. However, some bottlenecks such as high operation voltage, hysteresis, residual birefringence, charging issues due to the large capacitance, and relatively low transmittance remain to be overcome before their widespread applications can be realized. Recent progress on BPLC materials and devices has shown great promise. To realize the electro-optic effect of PS-BPLC, two driving modes: in-plane switching and vertical field switching mode, have been developed. The material system of PS-BPLC, including nematic LC host, chiral dopant, and polymer network, are discussed. Each component plays an essential role affecting the stability and electro-optic properties of PS-BPLC. © 2014 Wiley Periodicals, Inc. J. Appl. Polym. Sci. **2014**, *131*, 40556.

KEYWORDS: photopolymerization; liquid crystals; optical properties

Received 15 January 2014; accepted 3 February 2014
DOI: 10.1002/app.40556

INTRODUCTION

Blue phases (BPs)[1,2] exist between chiral nematic and isotropic phases. When the first such compound was discovered, it happened to appear blue color because of Bragg reflection. Therefore, it was termed blue phase liquid crystal (BPLC) since. For many applications, such as transmissive displays, the Bragg reflection is shifted to ultraviolet (UV) region so that such a BPLC is actually transparent in the visible region. With nanostructured double twist cylinders (DTCs) and self-assembled three-dimensional cubic lattice structures, blue phases are of interest in fast electro-optic components, tunable photonic crystals,[3] and three-dimensional lasers.[4] However, the narrow temperature range due to the frustration between the DTCs limits the application. In 1993, Kitzerow et al.[5] formed blue phases of polymeric liquid crystal monomers and polymerized these monomers while maintaining blue phase structure, leading to a solid resin of fixed blue-phase structure. Although this system maintains blue-phase structure, the liquid crystal cannot be dynamically switched because all the constituent molecules were polymerized. In 2002, Kikuchi et al.[6] successfully extended the BP temperature range to over 60°C including room temperature through polymer stabilization process. By refilling the blue phase templated polymer network with achiral nematic liquid crystal, Coles and coworkers[7] demonstrated a thermally stable blue phase from −125 to 125°C. Polymer-stabilized blue-phase liquid crystal (PS-BPLC)[6,8–12] opens a gateway for next-generation display and photonics applications.[13] With self-assembled microscopic structure, PS-BPLC exhibits three distinctive features: (1) self-assembly process so that no surfactant (e.g., polyimide layer) is needed to generate uniform molecular alignment, (2) nanoscale (∼100 nm) double-twist cylinder diameter and short coherence length which leads to microsecond response time,[14,15] and (3) three-dimensional lattice structure resulting in optically isotropic voltage-off state, provided that Bragg reflection is in the UV region. Therefore, BPLC holds promises for fast-response transmissive display,[10,11] reflective display,[16–18] and photonics applications.[19–21]

PROPERTIES OF PS-BPLC

Blue Phase Appearance

In general, blue phases appear in a highly twisted chiral nematic liquid crystal.[22] Depending on the structure, there are up to three blue phases: BPI, BPII, and BPIII. BPI shows body-centered cubic structure, BPII has simple cubic structure while BPIII exhibits the same symmetry as isotropic phase.[22] The local refractive index variation in the blue phase structure results in selective Bragg reflections. However, blue phases are not necessarily blue. The reflection wavelength is governed by the lattice structure as:[23]

Yuan Chen is a Ph.D. candidate at College of Optics and Photonics, UCF. She has 24 journal publications. Her research focuses on advanced organic and quantum dot materials, and devices for display and photonic applications. In 2013, she received IEEE Photonics Society Graduate Student Fellowship, SPIE educational scholarship, and SID distinguished student paper award.

Shin-Tson Wu is a Pegasus professor at College of Optics and Photonics, UCF. He is a Charter Fellow of the National Academy of Inventors, a Fellow of the IEEE, OSA, SID, and SPIE. He is a recipient of 2014 OSA Esther Hoffman Beller medal, 2011 SID Slottow-Owaki prize, 2010 OSA Joseph Fraunhofer award, 2008 SPIE G. G. Stokes award and 2008 SID Jan Rajchman prize. He was the founding chief editor of the IEEE/OSA Journal of Display Technology.

$$\lambda = \frac{2na}{\sqrt{h^2+k^2+l^2}}, \quad (1)$$

where h, k, and l are the Miller indices of a crystal plane, n and a denote average refractive index and lattice constant of blue phases. The lattice constant is related to the pitch length p. For BPI, $a=p$, while for BPII $a=p/2$.[23] As the pitch length decreases, the reflected color shifts from red, green to blue. When blue phase grows from isotropic phase without any electric field, multiple diffraction peaks can be observed from (110), (200), and (211) directions (with these lattice surfaces parallel to the substrate) of BPI.[23] This forms the characteristic platelet texture of blue phase, as shown in Figure 1(a,c,e).[18]

Electric Field Effect

Blue phase liquid crystal molecules are anisotropic and dynamically switchable by electric field (E), which attracts tremendous attention. There are different electric field effects on blue phases, such as lattice orientation effect, Kerr effect, lattice distortion, phase transition, and so on.[24–26] When the multidomain BP lattice is subject to a uniform electric field, the nonzero torque exerted on the blue phase lattice will rotate the lattice to the nearest stable position where the torque vanishes.[24] Thus, the electric field-induced monodomain blue phase with single Bragg reflection peak is created, as shown in Figure 1(b,d,f).[18] Blue phase texture could be changed and narrow band reflection color is generated. It is worth to mention that surface alignment[17] and surface free energy engineering[27] have also been demonstrated to induce monodomain blue phases.

Besides the lattice reorientation effect, blue phase liquid crystal is optically isotropic at a wavelength considerably longer than the Bragg reflection and can be treated as a Kerr media. When an electric field is applied, liquid crystal molecules tend to align with the electric field if the dielectric anisotropy $\Delta\varepsilon > 0$ (or perpendicular to the electric field if $\Delta\varepsilon < 0$). As a result, birefringence is induced. In the low field region, the induced birefringence can be described by Kerr effect as:

$$\Delta n_{\text{ind}} = \lambda K E^2, \quad (2)$$

where λ is the wavelength, E is the electric field, and K is the Kerr constant. Typically K is positive as positive $\Delta\varepsilon$ LCs are usually used. However, with negative $\Delta\varepsilon$ LCs, PS-BPLC with a negative Kerr constant has also been reported,[28] although its Kerr constant is relatively small because of the relatively small $|\Delta\varepsilon|$ (< 10) of the negative LC host.

To better describe the saturation phenomenon of the induced birefringence, Yan et al. [29] proposed the extended Kerr effect:

$$\Delta n_{\text{ind}} = \Delta n_{\text{sat}} \left(1 - \exp\left(-(E/E_s)^2\right)\right), \quad (3)$$

where Δn_{sat} is saturation birefringence and E_s is the saturation electric field. Kerr effect exhibits a fast response time (<1 ms) because of the short coherent length of BPLC. However, a higher electric field could lead to lattice distortion and hence Bragg reflection wavelength shift.[23] The relaxation time of lattice distortion is in the order of 10–100 ms. Under a sufficiently high electric field, blue phase may transform to new phases, to chiral nematic phases, and ultimately to nematic phases.[26,30] This transition is usually very slow (a few seconds or even longer), which causes undesirable hysteresis or residual birefringence.

In the case of PS-BPLC, local reorientation (Kerr effect) mostly occurs on application of the electric field, as the lattice structure is restricted by the polymer network.[8] The Bragg reflection color change under electric field should be very minor.[6] Figure 2 depicts the reflection spectra of a monodomain PS-BPLC cell (cell gap: 5 μm) under different applied voltages. The electric field-induced monodomain blue phase exhibits a fairly high reflectance and narrow bandwidth. The full width at half maximum of the reflection band is about 25 nm, so the appearance color is quite saturated and vivid. When an AC voltage is applied, the double-twist cylinders are gradually unwound, which leads to a decreased reflectance. Figure 2 depicts the reflection spectra at different operating voltages.[18] A tiny blue shift (< 5 nm) on the peak reflection wavelength is observed, indicating the lattice deformation of the PS-BPLC is small. If the electric field is strong enough, even the polymer network could be deformed.

Operation Voltage

PS-BPLC has many attractive features, however high operation voltage, noticeable hysteresis, and large capacitance still hinder

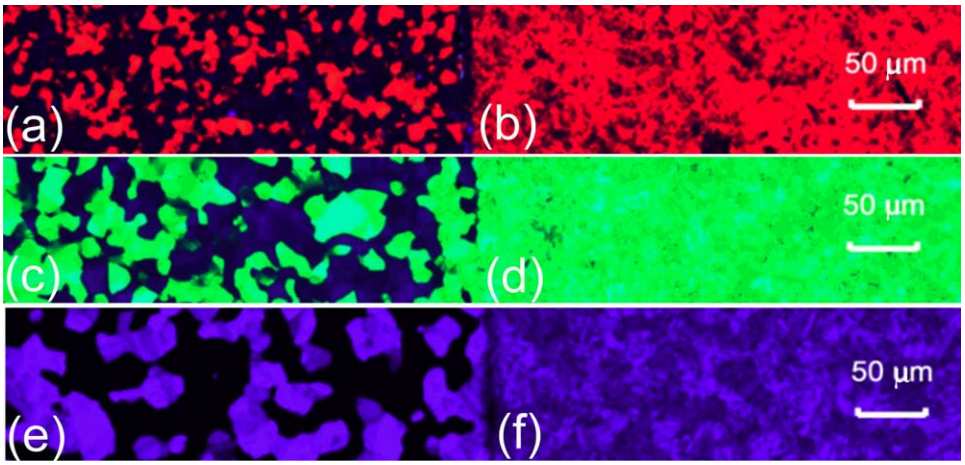

Figure 1. (a),(c),(e) Typical multi-domain blue phase platelet texture (b),(d),(e) monodomain blue phase texture with different pitch length. Reflective images. [Color figure can be viewed in the online issue, which is available at wileyonlinelibrary.com.]

its widespread applications. Among these three technical barriers, high voltage is the root cause. If the voltage is low (< 10 V), then the electrostriction effect, which causes lattice distortion would be suppressed, hysteresis would be negligible (< 1%), and moreover high frame rate (> 180 Hz) can be achieved by the bootstrapping circuits.[31] Therefore, the most fundamental issue for BPLC studies is to lower the operation voltage to below 10 V, without sacrificing other desirable properties, such as high transmittance, submillisecond response time, high contrast ratio, and wide viewing angle. To achieve this goal, both device structures and BPLC materials have been investigated extensively. From device structure viewpoint, two major approaches have been developed: (1) implementing protrusion electrodes so that the fringing field can penetrate deeply into the LC bulk,[32–34] and (2) vertical field switching (VFS)[35] to generate uniform longitudinal field across the BPLC layer. From material aspect, developing BPLC materials with a large Kerr constant (K)[36–38] helps reduce driving voltage because the on-state voltage is inversely proportional to $\sqrt{K}$.[32] From Gerber's model, Kerr constant is governed by the birefringence (Δn), dielectric anisotropy ($\Delta\varepsilon$), average elastic constant (k), and pitch length (p) of the chiral LC host as:[25]

$$K \approx \Delta n \Delta\varepsilon \frac{p^2}{\lambda k (2\pi)^2}. \quad (4)$$

Response Time

Fast response time is probably the most attractive feature for PS-BPLC. The relaxation time of a BPLC is determined by rotational viscosity (γ_1), elastic constant and pitch length as:[11]

$$\tau = \frac{\gamma_1 p^2}{k(2\pi)^2} \quad (5)$$

It is known that the BPLC response time in the low field region where lattice distortion does not occur is primarily governed by the viscosity, average elastic constant, and pitch length.[15,25,39] Polymer structure and polymer concentration also play important roles.[32]

All the properties are closely related to the PS-BPLC materials. We will discuss the material system of PS-BPLC and the contribution of each component to the physical properties in the following section.

PS-BPLC MATERIAL SYSTEM

A PS-BPLC precursor typically comprises of 70–90 wt % of nematic LC host as switching molecules, 5–10 wt % of chiral dopant to induce blue phase, and 8–15 wt % of photo-curable monomers and ~1% of photo initiator for polymer stabilization. Figure 3 shows the chemical structures of some nematic LC compounds, chiral dopants, and monomers.[40,41] The properties and influence of each component on the PS-BPLC will be described in details later. To form BPLC composite, the precursor is cooled from isotropic phase to blue phase, and then exposed to UV light. After UV irradiation, polymer-stabilized BPLC nano-composites are self-assembled, exhibiting the characteristic small platelet structures.

Nematic Liquid Crystal Host

A PS-BPLC typically consists of 70%–90% nematic liquid crystal host. As a major component, the properties of the LC host

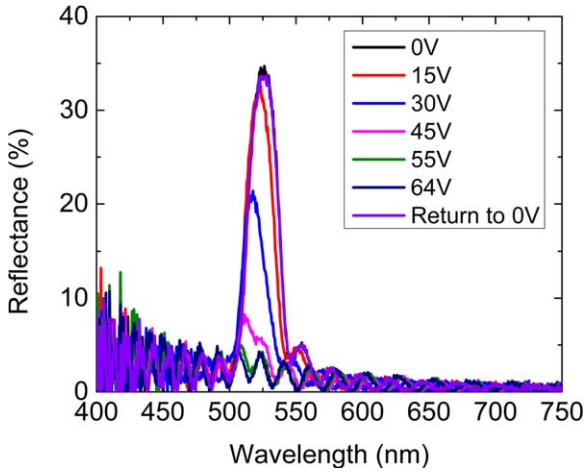

Figure 2. Bragg reflection spectra of a monodomain PS-BPLC cell under different voltages (cell gap: 5 μm). [Color figure can be viewed in the online issue, which is available at wileyonlinelibrary.com.]

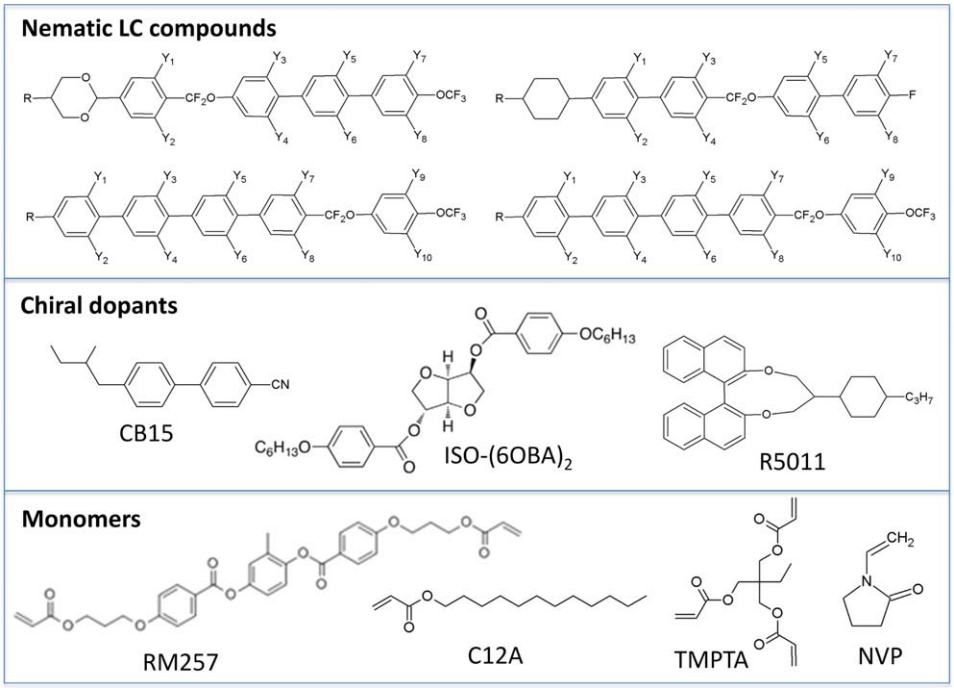

Figure 3. Chemical structures of some exemplary nematic LC hosts, chiral dopants, and monomers used in polymer-stabilized BPLC systems. [Color figure can be viewed in the online issue, which is available at wileyonlinelibrary.com.]

would significantly affect the properties of the PS-BPLC, e.g., Kerr constant and response time. Choi et al.[9] has experimentally demonstrated that Kerr constant is proportional to $\Delta n \Delta\varepsilon \cdot k_{33}/k_{11}$ of the nematic LC host. Besides, the viscosity and relaxation frequency of nematic LC host also significantly affect the performance of a PS-BPLC.

Birefringence. From eq. (1), a straightforward approach to increase Kerr constant is to boost $\Delta n \cdot \Delta\varepsilon$ because k of the LC host is more difficult to control.[9] The birefringence can be increased by elongating the liquid crystal molecular conjugation length. But the photo-stability and solubility of high birefringence LCs should be taken into consideration. Considering the material stability, melting temperature, and viscosity, terphenyl derivatives could be the longest conjugation for BPLCs. For a stable material, the birefringence is usually smaller than 0.28. It is challenging to get large K through increasing Δn alone. On the other hand, since Δn is wavelength dependent, λK also follows the same dispersion trend as its nematic host LC, and can be described well by the single-band birefringence dispersion model, as reported by Jiao et al.[42]

Dielectric Anisotropy. Increasing $\Delta\varepsilon$ is an effective approach to improve Kerr constant. Indeed, LC hosts with $\Delta\varepsilon$ (> 90) have been developed by JNC[36] and by Merck[37] independently. Figure 3 depicts some examples for large $\Delta\varepsilon$ LC compounds.[40] Such a large $\Delta\varepsilon$ LC would require several polar groups so that its rotational viscosity and response time would increase dramatically. Indeed, the response time of JC-BP01M is about 2 ms at room temperature (RT $\sim$ 22°C) using an in-plane switching (IPS) cell.[36] In addition, the hysteresis is about 6% because of the strong peak electric field near the IPS electrode edges. A delicate balance between operating voltage, response time, hysteresis, and relaxation frequency has to be taken into consideration.

Recently, Chen et al.[38] demonstrated a low voltage, submillisecond response time, and hysteresis-free PS-BPLC using a very large $\Delta\varepsilon$ ($\sim$470) LC host JC-BP06N (by JNC) whose clearing point is $T_c = 73.8$°C. The rotational viscosity of JC-BP06N is over 1470 mPa s due to the huge $\Delta\varepsilon$. The blue phase precursor consists of 88.17 wt % JC-BP06N with 2.92 wt % of chiral dopant R5011 (HCCH), 5.24 wt % RM257 (Merck), 3.46 wt % TMPTA (Sigma Aldrich), and 0.21 wt % photoinitiator. The BPLC precursor was filled into an LC cell without PI. Afterward, the cell was cooled to blue phase and then exposed to UV light ($\lambda \sim$ 365 nm) with intensity of 2 mW/cm^2 for 30 min. After UV irradiation, nano-structured BPLC composites were self-assembled. The measured Bragg reflection wavelength is $\sim$380 nm, which is about the same as that of JC-BP01M. To realize the electro-optic effect of BPLC, two device structures (IPS and VFS modes) are commonly used.

IPS mode. IPS mode is to use fringing field generated from interdigitated striped electrodes. The major advantages of IPS mode are threefold: (1) a conventional backlight can be used, (2) large cell gap tolerance, and (3) wide viewing angle can be obtained by a simple biaxial compensation film.[43] By using a large dielectric anisotropy LC, e.g., JC-BP06N, the driving voltage can be lower than 10V, depending on the electrode dimension. In experiment, we used an IPS-5/5 cell whose electrode width and gap are both 5 μm, and cell gap is 7 μm. The IPS cell was then sandwiched between two crossed polarizers and the voltage dependent transmitted light was focused by a lens so that different diffraction orders[13] can be collected by the detector. Figure 4(a) plots the normalized voltage-dependent

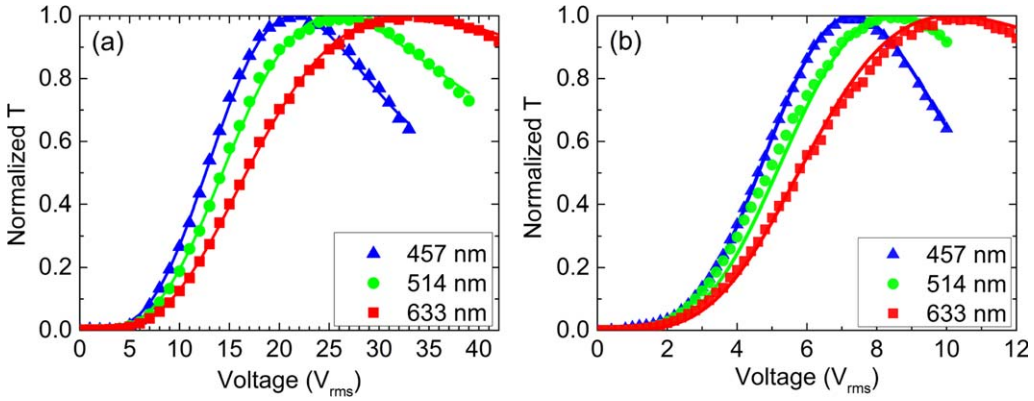

Figure 4. Normalized VT curves of the PSBP cells using JC-BP06N at the specified wavelengths. (a) IPS cell ($d = 7$ μm) and (b) VFS cell ($d = 3.2$ μm). Dots are measured data and lines are fitted curves with extended Kerr model. [Color figure can be viewed in the online issue, which is available at wileyonlinelibrary.com.]

transmittance (VT) curves at different wavelengths. The on-state voltage (corresponding to peak transmittance) $V_{on} = 22.2$, 25.4, and 32.8 V_{rms} at $\lambda = 457$, 514, and 633 nm, respectively. Through fitting the data with the extended Kerr model,[10,29] we get $K = 39.7$, 33.1, and 26.9 nm/V^2, correspondingly. By contrast, the Kerr constant of this BPLC is ~2.1× larger than that of JC-BP01M at room temperature (also in IPS cell).[44] The driving voltage of JC-BP06N BPLC in IPS cell is still not low enough and the peak transmittance of the IPS-5/5 cell is about 60%. For IPS, the non-uniformity in electric field, including dead zones on top of electrode, causes some transmittance loss. By reducing the width (w) and gap (l) of the IPS electrodes, the operation voltage is reduced while the transmittance keeping above 80%.[45] Reducing the ratio of w/l would also help to reduce the dead zone area ratio and improve the transmittance. A refraction model has been developed to better predict the transmittance of IPS BPLCD and promising approaches, such as etched electrode design, for achieving high transmittance and low operation voltage have been demonstrated.[12]

VFS mode. In VFS mode,[35] the electric field is in longitudinal direction. VFS mode offers several spectacular properties, such as low voltage, high transmittance, fast response time, and negligible hysteresis, but it requires a directional backlight and special phase compensation to achieve wide view.[46] To acquire phase retardation, the laser beam was incident on the VFS cell at 70° oblique angle. The VFS cell ($d = 3.2$ μm) was immersed in a transparent container filled with Glycerol ($n = 1.47$) so that the beam could enter the LC layer at a large angle due to the refractive index match between the glass and Glycerol.[35] The cell was driven at 100 Hz. The Kerr constant decreases as the driving frequency increases, following the extended Coles-Coles model.[47] Ideally, a driving frequency higher than 180 Hz is required for color sequential displays.[48] If the driving frequency was increased to 240 Hz, Kerr constant would drop by 8%, which in turn increase the on-state voltage by ~4%. This prediction was validated experimentally.

Figure 4(b) depicts the measured VT curve at different wavelengths. $V_{on} = 7.3$, 8.4, and 9.9 V_{rms} for $\lambda = 457$, 514, and 633 nm, respectively. In the voltage-off state, blue phase is not perfectly optically isotropic but with a tiny optically rotatory power.[49] At $\lambda = 514$ nm, the measured contrast ratio (CR, defined as the ratio of peak transmittance over light leakage at $V = 0$) is 580 : 1 under crossed polarizers. By simply rotating the analyzer by 1.8°, CR is boosted to 1900 : 1. The depolarization from the oblique incidence might also degrade CR. Through fitting the VT curves,[10] $K = \Delta n_s/(\lambda E_s^2) = 24.9$, 20.9, and 17.4 nm/V^2 for $\lambda = 457$, 514, and 633 nm, respectively. For comparison, at $\lambda = 633$ nm the Kerr constant of our BPLC is ~2.3× larger than that of JC-BP01M (also from VFS cell). This improvement is close to 2.1× by using the IPS cells, considering the measurement and fitting errors. So, on average our PS-BPLC shows a 2.2× larger Kerr constant than JC-BP01M. For VFS BPLCD, the peak transmittance of the cell is approaching 100%. However, the sophisticated phase compensation and optical design[50] decreases the transmittance to ~85%. Optimization in the design is needed.

Viscosity. With such a large $\Delta\varepsilon$, the rotational viscosity of the nematic LC for PS-BPLC would be inevitably high due to the addition of several polar groups. For example, at room temperature the rotational viscosity of JC-BP06N is over 1470 mPa s, which is about 7× higher than that of Merck E7 ($\gamma_1 \sim 200$ mPa s). Fast response time is one of the major attractions of PS-BPLC devices. However, if the BPLC is too viscous the response time could be relatively slow (~2 ms), according to eq. (5). Diluters have been widely used for lowering the viscosity and melting temperature of a nematic LC.[51–57] The diluter effects have also been investigated on polymer-stabilized BPLC.[58] A small amount of diluter slightly decreases the birefringence and dielectric anisotropy, but it dramatically reduces the viscosity of the LC host. For example, by doping 6% of 5CC3 [4-pentyl-4′-propyl-1,1′-bi(cyclohexyl)] into a viscous LC host (HTG-135200, HCCH), the rotational viscosity γ_1 is reduced by 200% at 25°C, Δn by 6%, and $\Delta\varepsilon$ by 10%. The decay time of the resultant PS-BPLC could be reduced by 2×–3× while keeping the Kerr constant unchanged. The decay time was measured between 90% and 10% transmittance change at 25°C. The measured decay time of PSBP without diluter is 1700 μs. After adding a diluter, the decay time is reduced by 2×–3×.

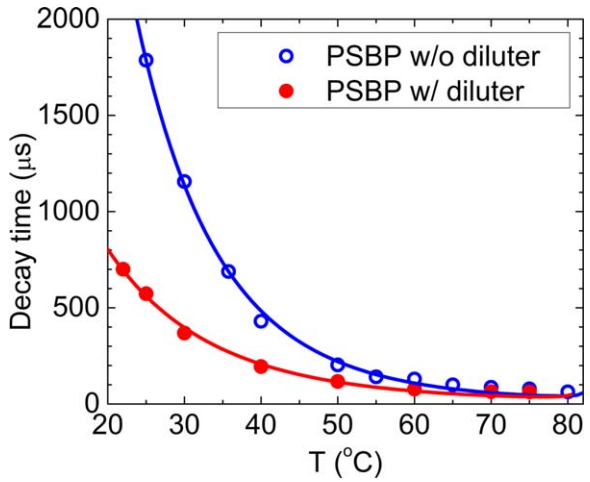

Figure 5. Temperature dependent response time of a PSBP with and without diluter. LC host: HTG-135200, diluter: 6% 5CC3, BPLC cell: IPS mode. [Color figure can be viewed in the online issue, which is available at wileyonlinelibrary.com.]

To investigate the activation energy, which is related to the viscosity of the PSBP, we measured the temperature dependent decay time of PSBP with/without diluter. Results are shown in Figure 5. The decay time decreases as the temperature increases, as described by following equation:[59]

$$\tau \approx B \cdot \frac{\exp\left(E_a/k_B T\right)}{\left(1-T/T_{c_B P}\right)^{\beta}}, \tag{6}$$

where B is a proportionality constant, E_a is the activation energy of the PSBP, and T_{c_BP} is the clearing point of the PS-BPLC. The material constant β has been obtained from the LC host.[58] From fittings, we obtained $E_a = 738$ meV and $B = 4.0{\cdot}10^{-10}$ μs for PSBP without diluter, and $E_a = 573$ meV, $B = 7.8{\cdot}10^{-8}$ μs for PSBP with diluter. As expected, PSBP with diluter has lower activation energy, since the diluter helps to make the PSBP less viscous. Moreover, PS-BPLC has a higher activation energy than the nematic LC host, indicating that the added chiral dopant also increases the viscosity.

Relaxation Frequency. Since the relaxation frequency f_r is proportional to $1/(\eta l^3)$,[60] a large $\Delta\varepsilon$ LC would lead to a fairly low relaxation frequency; e.g., JNC JC-BP01M has a relaxation frequency of 1.3 kHz, and its Kerr constant decreases by ~2× as the frequency increases from 60 Hz to 1 kHz.[47] When driving this BPLC at 1 kHz for color sequential displays, two serious problems are encountered: (1) the operation voltage is increased by ~40%, and (2) the dielectric heating effect[61–63] due to the imaginary part (absorption) of dielectric constant, which has a peak value at the relaxation frequency, will affect the performance stability of the BPLC device. An effective diluter would help to dramatically reduce the viscosity and increase the relaxation frequency.

Figure 6 depicts the measured $\varepsilon'_{\perp}$ and $\varepsilon'_{//}$ (real part of the permittivity) of JC-BP06N. Dots are the measured $\varepsilon'_{//}$ for JC-BP06N and lines are fitting results with Debye relaxation equation:[64,65]

$$\varepsilon'_{//} = \varepsilon_\infty + \frac{\varepsilon_0 - \varepsilon_\infty}{1+(f/f_r)^2} \tag{7}$$

From these data, we obtain $\varepsilon_0 = 491$ at low frequency region for JC-BP06N. As the frequency increases, $\varepsilon'_{//}$ decreases dramatically due to the slow dielectric relaxation time resulting from the large viscosity and bulky molecular structure.[60] Through fitting with eq. (7), we find $f_r = 1.07$ kHz. For conventional nematic LCs, the relaxation frequency is usually quite high (> 50 kHz). After doping a small amount of diluter (5 wt % of 5CC3), f_r shifts to 1.92 kHz because of the dramatically reduced viscosity.[58] However, ε_0 drops nonlinearly from 491 to 311 after adding 5 wt % 5CC3.[38,66]

Moreover, the relaxation frequency decreases exponentially with temperature. Thus, low temperature and high frequency operation for large viscosity PS-BPLCs would be limited.[45] Even the temperature is still above the melting point of a blue phase (ultimate limit), the dramatic plunge of $\Delta\varepsilon$ results in a tremendously high driving voltage, which makes the device difficult to operate. Again, an effective diluter would help to increase the relaxation frequency and benefit the low temperature operation.[58]

Chiral Dopants

Chiral dopants are essential to introduce high chirality to the nematic LC host and induce blue phases. The pitch length p is inversely proportional to the HTP (helical twisting power, which could vary slightly depending on the nematic LC host) and concentration (c) of the chiral dopant as $p = 1/(\text{HTP}^*c)$. Thus we can tune the pitch length and hence Bragg reflection wavelength by choosing different chiral dopants or varying the concentration of the chiral dopant. If a chiral dopant has a weaker HTP, then its concentration should be increased, leading to some disadvantages: (a) The corresponding ratio of nematic LC host (switching molecules) would be lower, which could result in a smaller Kerr constant; (b) Most chiral dopants do not have mesongenic phase, therefore adding more chiral dopant would decrease the clearing point of the BPLC; (3) The solubility of the chiral dopant is usually limited: a too high concentration might cause saturation in pitch length or even

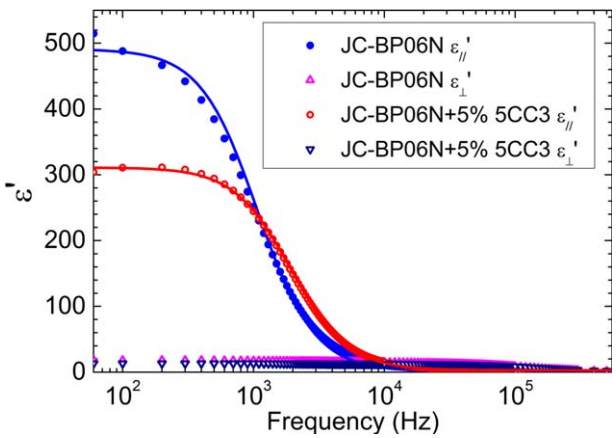

Figure 6. Frequency-dependent $\varepsilon'_{//}$ and $\varepsilon'_{\perp}$ of JC-BP06N before and after adding 5% 5CC3. [Color figure can be viewed in the online issue, which is available at wileyonlinelibrary.com.]

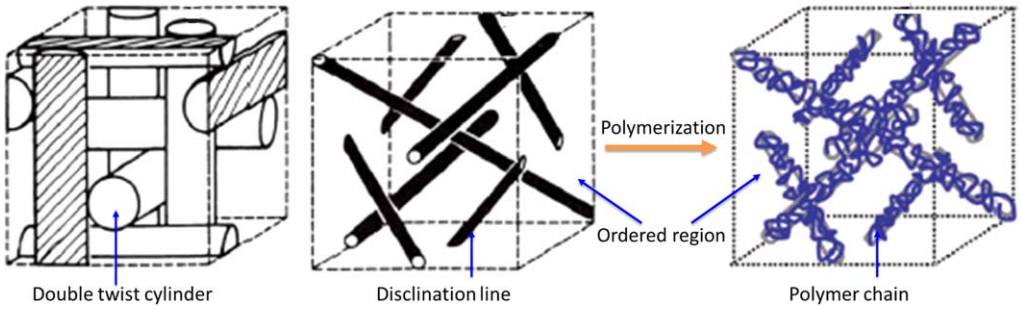

Figure 7. Illustration of the mechanism for polymer stabilization effect on blue phase. [Color figure can be viewed in the online issue, which is available at wileyonlinelibrary.com.]

precipitation. As a result, the stability of the PS-BPLC will be affected. The HTP value of some commercial chiral dopants is relatively low, i.e., HTP $\sim$ 8/μm for CB15. However for BPLC, a high HTP chiral dopant, such as R5011 (HTP > 100/μm, whose structure is shown in Figure 3) has been commonly used.[41]

For transmissive displays, the Bragg reflection of blue phases is shifted into UV region (< 380nm) to obtain an optically isotropic state in the visible region. A shorter Bragg reflection wavelength helps to improve the CR.[15] However, blue phase is not perfectly optically isotropic but with a tiny optical rotatory power.[49] Based on this property, approaches have been proposed to compensate the light leakage and thereby improve the contrast ratio and widen the viewing angle of a BPLC display.[67]

As shown in eq. (4), the Kerr constant is proportional to the square of pitch length. Kikuchi and coworkers[68,69] experimentally demonstrated that the Kerr constant increases significantly with the increased pitch length. By shifting the Bragg reflection from 350 nm to 600 nm, the Kerr constant was improved and the on-state voltage reduced by 35%, as reported by Yan et al.[17] In principle, we can even shift the Bragg reflection to near infrared region. However, some problems associated with this long-pitch approach are found: (1) To retain high contrast ratio, two circular polarizers have to be used. A circular polarizer is usually comprised of a linear polarizer and a quarter-wave plate so that its cost is more expensive. (2) The long-pitch BPLC leads to slower response time as Gerber's model predicts. (3) A longer pitch length implies to a lower chirality and blue phases may no longer exist. (4) Higher order Bragg reflection could appear in the visible region, which would degrade the contrast ratio. The Bragg reflection wavelength can be intentionally tuned to a visible wavelength for reflective display[17,18] or laser applications.[70]

The handedness of the chiral dopant also plays an interesting role on the physical properties of PS-BPLC. Chen and Wu[18] investigated the polarization ellipse of the reflected light for both RCP and LP incident lights for an electric field-induced monodomain BPLC. With a right-handed chiral dopant, the reflected light has right-handed circular polarization for both RCP and LP incident beams. The ellipticity ε is defined as the ratio of the major axis to the minor axis of the polarization ellipse. $\varepsilon = 0$ or ∞ represents LP and $\varepsilon = 1$ means circular polarization. The measured ε of the reflected light is 0.985 and 0.991 for the RCP and LP incident lights, respectively, indicating the reflected light is very close to circularly polarized, regardless of the polarization state of the incident light. The agreement between the handedness of the chiral dopant and reflection polarization from PS-BPLC has also been reported elsewhere.[7,17]

Polymer Network

As shown in Figure 7, BPLC has DTC structures and these cylinders will further form periodic lattice. When these DTCs are in contact, there are disclination lines. Blue phases must coexist with disclinations for topological reasons, which maintains the balance of BP thermodynamically.[23] Due to the defect lines, BP only exists in a narrow temperature range. Polymer networks play a key role in the PSBP system as they concentrate on the disclination core in a random coil conformation in the lattice structures and stabilize the blue phases.[6] Certain amount of monomers is needed to expand the temperature range. Typically, a diacrylate monomer (e.g., RM257) and a monofunctional monomer (C12A) or tri-functional monomer (TMPTA) are jointly used to stabilize a blue phase. The chemical structures for these monomers are shown in Figure 3. After polymerization, the miscibility of the polymer chains with liquid crystal molecules cannot be too high, otherwise, the polymer would be homogeneously dispersed in the liquid crystal, and there is no stabilization effect.[6] With Confocal Laser Scanning Microscope, Kikuchi and coworkers[71] have directly observed the periodic pattern images of PS-BPLC, due to (110), (100), (111), and (211) planes of BCC lattice in BPI.

Besides temperature stability, polymer network also influences the electro-optic properties. Increasing monomer concentration in a certain range leads to higher operating voltage, smaller hysteresis, lower residual birefringence, and faster response time.[72,73] The copolymerization reactivity ratio of two different monomers, and types of monomers would also change the formation of the polymer network.

To compare the influence of the polymer network on the electro-optic properties of PS-BPLC, we prepared two samples with different monomer compositions. Sample A used C12A while Sample B used TMPTA. For each sample, 10 wt % of monomers [6 wt % RM257 (Merck) + 4 wt % C12A or TMPTA] and 0.8 wt % of photoinitiator were blended with 89.2 wt % of the BP host (93% JM2069-145, ITRI Taiwan and

Table I. Comparison between Sample A and Sample B

	Compositions							Hysteresis		
Sample	BP host	RM257	C12A	TMPTA	PI	V_{on} (V)	K (nm/V^2)	Drive to 35.8 V	Drive to 44 V	Decay time (μs)
A	89.2 wt %	6 wt %	4 wt %	0	0.8 wt %	35.8	0.97	~0	1.8%	332.5
B	89.2 wt %	6 wt %	0	4 wt %	0.8 wt %	44.2	0.6	~0	0.68%	39.4

7% R5011) to form the precursors. After UV irradiation, polymer-stabilized BPLC nano-composites were self-assembled. We then measured their electro-optic properties.

For Sample B, the transmission peak occurs at $V_p = 44.2$ V, which corresponds to an electric field of 8.39 V/μm. Through fitting,[10] we obtained the Kerr constant $K = \Delta n_s/(\lambda E_s^2) = 0.6$ nm /V^2. By contrast, the on-state voltage of Sample A is 35.8 V and the Kerr constant is 0.97 nm/V^2. As the pitch length, Δn and $\Delta\varepsilon$ are the same for both samples, we find that the elastic constant of Sample B is 1.6× larger than that of Sample A. The increased elastic constant is believed to originate from the strong polymer network[74,75] formed with RM257 and TMPTA which has three functional groups while C12A only has one. A strong polymer network helps to reduce hysteresis and response time.

Hysteresis affects gray scale accuracy of a BPLC device and should be minimized[76] and it is also a great way to characterize the rigidness of the polymer network. To measure hysteresis, we drove the cell by ascending the voltage to V_p and then gradually descending it to 0. Hysteresis is defined as $\Delta V/V_p$, where ΔV is the voltage difference between the forward and backward scans at half of the peak transmittance. For Sample B, the measured $\Delta V/V_p$ is only 0.68%. Although the maximum electric field is as strong as 8.39 V/μm, the hysteresis is still negligible, indicating the polymer network is quite stable.[77] If the cell is driven to 31 V (i.e., 50% of the peak transmittance) and then back to zero, hysteresis is too small (< 0.1%) to be detected by our measurement system. For Sample A, the hysteresis is free when driving to its peak voltage of 35.8 V but increases to 1.8% when driving to 44.2 V. This again indicates that the polymer network with TMPTA is stronger than that with C12A. The comparison between Sample A and B is listed in Table I.

Fast response time is probably the most attractive feature for BPLC and it is also closely related to the polymer network. The decay time at room temperature (21°C) for Sample A is 332.5 μs, and rise time is 541.9 μs. On the other hand, Sample B exhibits much faster response, with 39.4 μs decay time, and 46 μs rise time. We believe that the fast response time originates from the short pitch length and strong polymer network. TMPTA is a tri-functional monomer, while the normally used EHA or C12A[78] are mono-functional monomers. The crosslink between TMPTA and RM257 is much stronger, which helps the molecules to relax back when the voltage is released, indicating a much larger elastic constant.[74] In addition, the decay time decreases as the temperature increases. With TMPTA, we have demonstrated a microsecond response PS-BPLC.[15] As the temperature increases from 25.4°C to 44.3°C, the peak voltage increases slightly from 44.2 V to 50 V because of the reduced Kerr constant. Meanwhile, the decay time is reduced from 32.8 μs to 9.63 μs.

By doping a low molecular weight monomer (*N*-vinylpyrrollidone, NVP)[79,80] into a conventional BPLC system (with RM257 and TMPTA), Zhu et al.[81] found that the resultant Kerr constant is increased by 54% while response time shortened by 23%. A reactive diluent can be formed by NVP and acrylic functional groups of the RM257 and TMPTA after polymerization. It can degrade the strength of polymer network and reduce the interfacial energy at the interface between the polymer network and DTCs that increase the Kerr constant.[82] Meanwhile, it helps to reduce the effective rotational viscosity of the material system resulting in faster response time of PS-BPLC.

Besides the monomer composition and concentration, the polymerization conditions also affect the formation of the polymer network, such as curing temperature, exposure wavelength and intensity of UV light and so on.[83,84] To better understand and elaborate the mechanism of polymer network formation under different conditions and the effects on the corresponding electro-optic properties of PS-BPLC, further experimental investigations are necessary.

CONCLUSION AND OUTLOOKS

We have briefly reviewed the material system and electro-optic properties of polymer-stabilized blue phase liquid crystals from application viewpoint. The compositions of PS-BPLC, including nematic LC host, chiral dopant, and polymer network, are discussed. Each component plays an essential role in affecting the stability and electro-optic properties of PS-BPLC. With wide stable temperature range, submillisecond response time, and optically isotropic dark state, PS-BPLC is emerging as a promising candidate for next-generation display and photonics devices. With rapid advances in PS-BPLC materials and device structures, the driving voltage has been reduced to < 10 V, while maintaining submillisecond response time, high contrast ratio, and negligible hysteresis. This paves the way for future widespread application of PS-BPLCs.

ACKNOWLEDGMENTS

The authors are indebted to ITRI (Taiwan) and AUO for financial support.

REFERENCES

1. Reinitzer, F. *Monatsh. Chem.* **1888**, *9*, 421.
2. Yoshizawa, A. *RSC Adv.* **2013**, *3*, 25475.

3. Etchegoin, P. *Phys. Rev. E* **2000**, *62*, 1435.
4. Cao, W. Y.; Munoz, A.; Palffy-Muhoray, P.; Taheri, B. *Nat. Mater.* **2002**, *1*, 111.
5. Kitzerow, H. S.; Schmid, H.; Ranft, A.; Heppke, G.; Hikmet, R. A. M.; Lub, J. *Liq. Cryst.* **1993**, *14*, 911.
6. Kikuchi, H.; Yokota, M.; Hisakado, Y.; Yang, H.; Kajiyama, T. *Nat. Mater.* **2002**, *1*, 64.
7. Castles, F.; Day, F. V.; Morris, S. M.; Ko, D. H.; Gardiner, D. J.; Qasim, M. M.; Nosheen, S.; Hands, P. J. W.; Choi, S. S.; Friend, R. H.; Coles, H. *J. Nat. Mater.* **2012**, *11*, 599.
8. Hisakado, Y.; Kikuchi, H.; Nagamura, T.; Kajiyama, T. *Adv. Mater.* **2005**, *17*, 96.
9. Choi, S. W.; Yamamoto, S.; Haseba, Y.; Higuchi, H.; Kikuchi, H. *Appl. Phys. Lett.* **2008**, *92*, 043119.
10. Ge, Z.; Gauza, S.; Jiao, M.; Xianyu, H.; Wu, S. T. *Appl. Phys. Lett.* **2009**, *94*, 101104.
11. Yan, J.; Rao, L.; Jiao, M.; Li, Y.; Cheng, H. C.; Wu, S. T. *J. Mater. Chem.* **2011**, *21*, 7870.
12. Xu, D.; Chen, Y.; Liu, Y.; Wu, S. T. *Opt. Express* **2013**, *21*, 24721.
13. Yan, J.; Li, Y.; Wu, S. T. *Opt. Lett.* **2011**, *36*, 1404.
14. Chen, K. M.; Gauza, S.; Xianyu, H.; Wu, S. T. *J. Display Technol.* **2010**, *6*, 49.
15. Chen, Y.; Yan, J.; Sun, J.; Wu, S. T.; Liang, X.; Liu, S. H.; Hsieh, P. J.; Cheng, K. L.; Shiu, J. W. *Appl. Phys. Lett.* **2011**, *99*, 201105.
16. Lin, Y. H.; Chen, H. S.; Chiang, T. H. *J. Soc. Inf. Disp.* **2012**, *20*, 333.
17. Yan, J.; Wu, S. T.; Cheng, K. L.; Shiu, J. W. *Appl. Phys. Lett.* **2013**, *102*, 081102.
18. Chen, Y.; Wu, S. T. *Appl. Phys. Lett.* **2013**, *102*, 171110.
19. Li, Y.; Wu, S. T. *Opt. Express* **2011**, *19*, 8045.
20. Lin, Y. H.; Chen, H. S.; Lin, H. C.; Tsou, Y. S.; Hsu, H. K.; Li, W. Y. *Appl. Phys. Lett.* **2010**, *96*, 113505.
21. Coles, H. J.; Morris, S. *Nat. Photonics* **2010**, *4*, 676.
22. Kitzerow, H. S.; Bahr, C. Chirality in Liquid Crystals; Springer: New York, **2001**.
23. Kikuchi, H. Liquid Crystalline Blue Phases; Springer Berlin: Heidelberg, **2008**.
24. Pieranski, P.; Cladis, P. E.; Garel, T.; Barbetmassin, R. *J. Physique* **1986**, *47*, 139.
25. Gerber, P. R. *Mol. Cryst. Liq. Cryst.* **1985**, *116*, 197.
26. Kitzerow, H. S. *Mol. Cryst. Liq. Cryst.* **1991**, *202*, 51.
27. Yamamoto, S.; Haseba, Y.; Higuchi, H.; Okumura, Y.; Kikuchi, H. *Liq. Cryst.* **2013**, *40*, 639.
28. Li, Y.; Chen, Y.; Yan, J.; Liu, Y. F.; Cui, J. P.; Wang, Q. H.; Wu, S. T. *Opt. Mater. Express* **2012**, *2*, 1135.
29. Yan, J.; Cheng, H. C.; Gauza, S.; Li, Y.; Jiao, M.; Rao, L.; Wu, S. T. *Appl. Phys. Lett.* **2010**, *96*, 071105.
30. Stegemeyer, H.; Porsch, F. *Phys. Rev. A.* **1984**, *30*, 3369.
31. Tu, C. D.; Lin, C. L.; Yan, J.; Chen, Y.; Lai, P. C.; Wu, S. T. *J. Display Technol.* **2013**, *9*, 3.
32. Rao, L.; Ge, Z.; Wu, S. T.; Lee, S. H. *Appl. Phys. Lett.* **2009**, *95*, 231101.
33. Kim, M.; Kim, M. S.; Kang, B. G.; Kim, M. K.; Yoon, S.; Lee, S. H.; Ge, Z.; Rao, L.; Gauza, S.; Wu, S. T. *J. Phys. D: Appl. Phys.* **2009**, *42*, 235502.
34. Jiao, M.; Li, Y.; Wu, S. T. *Appl. Phys. Lett.* **2010**, *96*, 011102.
35. Cheng, H. C.; Yan, J.; Ishinabe, T.; Wu, S. T. *Appl. Phys. Lett.* **2011**, *98*, 261102.
36. Rao, L.; Yan, J.; Wu, S. T.; Yamamoto, S. I.; Haseba, Y. *Appl. Phys. Lett.* **2011**, *98*, 081109.
37. Wittek, M.; Tanaka, N.; Wilkes, D.; Bremer, M.; Pauluth, D.; Canisius, J.; Yeh, A.; Yan, R.; Skjonnemand, K.; Klasen-Memmer, M. *SID Int. Symp. Digest Tech.* **2012**, *43*, 25.
38. Chen, Y.; Xu, D.; Wu, S. T.; Yamamoto, S.; Haseba, Y. *Appl. Phys. Lett.* **2013**, *102*, 141116.
39. Yan, J.; Wu, S. T. *J. Disp. Technol.* **2011**, *7*, 490.
40. Haseba, Y.; Kuninobu, T. Optically Isotropic Liquid Crystal Medium and Optical Device, U.S. Pat. 7,879,413 B2 (Feb. 1, **2011**).
41. Kirsch, A. P.; Pauluth, D.; Krause, J.; Heckmeier, M. Chiral Compounds, U.S. Pat. 7,223,150 B2 (May 29, **2007**).
42. Jiao, M.; Yan, J.; Wu, S. T. *Phys. Rev. E* **2011**, *83*, 041706.
43. Zhu, X.; Ge, Z.; Wu, S. T. *J. Display Technol.* **2006**, *2*, 2.
44. Rao, L.; Yan, J.; Wu, S. T.; Yamamoto, S.; Haseba, Y. *Appl. Phys. Lett.* **2011**, *98*, 081109.
45. Peng, F.; Chen, Y.; Chen, H.; Yuan, J.; Wu, S. T. *J. Mater. Chem. C*, DOI:10.1039/C4T00115J.
46. Cheng, H. C.; Yan, J.; Ishinabe, T.; Lin, C. H.; Liu, K. H.; Wu, S. T. *J. Display Technol.* **2012**, *8*, 627.
47. Li, Y.; Chen, Y.; Sun, J.; Wu, S. T.; Liu, S. H.; Hsieh, P. J.; Cheng, K. L.; Shiu, J. W. *Appl. Phys. Lett.* **2011**, *99*, 181126.
48. Bos, P.; Buzak, T.; Vatne, R. *Proc. SID* **1985**, *26*, 157.
49. Liu, Y.; Lan, Y. F.; Zhang, H.; Zhu, R.; Xu, D.; Tsai, C. Y.; Lu, J. K.; Sugiura, N.; Lin, Y. C.; Wu, S. T. *Appl. Phys. Lett.* **2013**, *102*, 131102.
50. Yan, J.; Xu, D.; Cheng, H. C.; Wu, S. T.; Lan, Y. F.; Tsai, C. Y. *Appl. Opt.* **2013**, *52*, 8840.
51. Heckmeier, M.; Pauluth, D. Liquid-Crystal Medium having a Low Threshold Voltage, U.S. Pat. 7,033,651 B2 (Apr. 25, **2006**).
52. Yanai, M.; Kubo, Y.; Nakagawa, E. Liquid Crystal Composition and Liquid Crystal Display Device, U.S. Pat. 6,572,938 B2 (Jun. 3, **2003**).
53. Hattori, N.; Yamamoto, H.; Fujita, H. Liquid Crystal Composition and Liquid Crystal Display Device, U.S. Pat. 7,608,310 B2 (Oct. 27, **2009**).
54. Schadt, M.; Buchecker, R.; Leenhouts, F.; Boller, A.; Villiger, A.; Petrzilka, M. *Mol. Cryst. Liq. Cryst.* **1986**, *139*, 1.
55. Schadt, M.; Buchecker, R.; Müller, K. *Liq. Cryst.* **1989**, *5*, 293.
56. Sun, J.; Xianyu, H.; Gauza, S.; Wu, S. T. *Liq. Cryst.* **2009**, *36*, 1401.
57. Song, Q.; Gauza, S.; Sun, J.; Wu, S. T.; Liang, X. *Liq. Cryst.* **2009**, *36*, 865.
58. Chen, Y.; Yan, J.; Schadt, M.; Liu, S. H.; Cheng, K. L.; Shiu, J. W.; Wu, S. T. *J. Display Technol.* **2013**, *9*, 592.

59. Rao, L.; Yan, J.; Wu, S. T. *J. Soc. Inf. Disp.* **2010**, *18*, 954.
60. Blinov, L. M. Electro-Optical and Magneto-Optical Properties of Liquid Crystals; Wiley: New York, **1983**.
61. Metaxas, A. C.; Meredith, R. J. Industrial Microwave Heating; IET: London, **1983**.
62. Schadt, M. *Mol. Cryst. Liq. Cryst.* **1981**, *66*, 639.
63. Wen, C. H.; Wu, S. T. *Appl. Phys. Lett.* **2005**, *86*, 231104.
64. Frank, F. C. *Discuss. Faraday Soc.* **1958**, *25*, 19.
65. Xianyu, H.; Wu, S. T.; Lin, C. L. *Liq. Cryst.* **2009**, *36*, 717.
66. Dakin, T. W. In Engineering Dielectrics; Bartnikas, R.; Eichhorn, R. M.; Brook, B., Eds.; ASTM International: Beltimore, **1983**; Chapter 8.
67. Liu, Y.; Lan, Y. F.; Hong, Q.; Wu, S. T. *J. Display Technol.* **2014**, *10*, 3.
68. Choi, H.; Higuchi, H.; Kikuchi, H. *Appl. Phys. Lett.* **2011**, *98*, 131905.
69. Choi, H.; Higuchi, H.; Kikuchi, H. *Soft Matter* **2011**, *7*, 4252.
70. Yokoyama, S.; Mashiko, S.; Kikuchi, H.; Uchida, K.; Nagamura, T. *Adv. Mater.* **2006**, *18*, 48.
71. Higashiguchi, K.; Yasui, K.; Kikuchi, H. *J. Am. Chem. Soc.* **2008**, *130*, 6326.
72. Mizunuma, T.; Oo, T. N.; Nagano, Y.; Ma, H.; Haseba, Y.; Higuchi, H.; Okumura, Y.; Kikuchi, H. *Opt. Mater. Express* **2011**, *1*, 1561.
73. Yan, J.; Wu, S. T. *J. Display Technol.* **2011**, *7*, 490.
74. Sun, J.; Xianyu, H.; Chen, Y.; Wu, S. T. *Appl. Phys. Lett.* **2011**, *99*, 021106.
75. Sun, J.; Wu, S. T. *J. Polym. Sci. Part B: Polym. Phys.* **2014**, *52*, 183.
76. Chen, K. M.; Gauza, S.; Xianyu, H.; Wu, S. T. *J. Display Technol.* **2010**, *6*, 318.
77. Rao, L.; Yan, J.; Wu, S. T.; Lai, Y. C.; Chiu, Y. H.; Chen, H. Y.; Liang, C. C.; Wu, C. M.; Hsieh, P. J.; Liu, S. H.; Cheng, K. L. *J. Display Technol.* **2011**, *7*, 627.
78. Yan, J.; Wu, S. T. *Opt. Mater. Express* **2011**, *1*, 1527.
79. Bunning, T. J.; Natarajan, L. V.; Tondiglia, V. P.; Sutherland, R. *Annu. Rev. Mater. Sci.* **2000**, *30*, 83.
80. Pogue, R.; Natarajan, L.; Siwecki, S.; Tondiglia, V.; Sutherland, R.; Bunning, T. *Polymer* **2000**, *41*, 733.
81. Zhu, J.; Ni, S.; Song, Y.; Zhong, E.; Wang, Y.; Chen, C.; Ye, Z.; He, G.; Wu, D.; Song, X.; Lu, J.; Su, Y. *Appl. Phys. Lett.* **2013**, *102*, 071104.
82. Zhu, J.; Ni, S.; Zhong, E.; Lu, J.; Su, Y. *SID Int. Symp. Digest Tech.* **2012**, *43*, 106.
83. Fan, C. Y.; Jau, H. C.; Lin, T. H.; Yu, F. C.; Huang, T. H.; Liu, C.; Sugiura, N. *J. Display Technol.* **2011**, *7*, 615.
84. Oo, T. N.; Mizunuma, T.; Nagano, Y.; Ma, H.; Ogawa, Y.; Haseba, Y.; Higuchi, H.; Okumura, Y.; Kikuchi, H. *Opt. Mater. Express* **2011**, *1*, 1502.